Identification of gastric cancer by fuzzy knowledge bases in the system of polarization reconstruction and analysis of the crystal structure of blood plasma

Nataliia I. Zabolotna*[a], Oleh V. Vlasenko[b], Vladyslava V. Sholota[a], Paweł Komada[c], Lyudmila V. Krylik[a], Alona A. Kolomiiets[a], Maktagali Bektemessov[d], Katarzyna Klimek[e]
[a]Vinnytsia National Technical University, Vinnytsia, Ukraine; [b]Vinnytsia Mykhailo Kotsiubynskyi State Pedagogical University, Vinnytsia, Ukraine; [c]Lublin University of Technology, Lublin, Poland; [d]Institute of Information and Computational Technologies CS MES RK, Almaty, Kazakhstan; [e]University Clinical Hospital No. 1, Lublin, Poland

ABSTRACT

The article shows the possibility of increasing the diagnostic accuracy of polarization methods for detecting human gastric cancer by analyzing the crystal structure of blood plasma with identification of the disease by fuzzy knowledge bases. A scheme of the system of polarization direct reconstruction of collections of orientational and phase-determined maps of blood plasma with analysis and classification in the diagnosis of gastric cancer is presented. A fuzzy expert knowledge base was provided in the form of estimates of statistical, correlation and spectral moments of collections of orientational and phase deterministic maps of blood plasma for normal conditions and gastric cancer. Fuzzy logic equations based on them were derived. The accuracy of diagnosis based on orientation and phase maps was achieved at the level of 86% and 92%, respectively.

Keywords: polarization reconstruction system, gastric cancer diagnostics, blood plasma, orientational deterministic maps, phase deterministic maps, fuzzy knowledge base

1. INTRODUCTION

Laser imaging polarimetry of blood plasma (BP) plays an important role in the early diagnosis of diseases of human internal organs[1–6]. Thus, based on visualization and objective analysis of the parameters of polarization images of BP, elements of the Muller and Jones matrices of BP, malignant diseases of the breast, cervical cancer , ovarian cancer, stomach cancer are diagnosed with high reliability. At the same time, minimal traumatism of patients is achieved in comparison with the methods of histopathological research. Based on the isotropic-anisotropic model of BP, the genesis of tumor processes is accompanied by changes in the albumin-globulin crystalline orientational-phase structure of blood plasma[1,5,6]. Changes in the orientation of the axes of albumin crystals are reflected in the orientational polarization maps of BP[7, 8].The elements of the phase polarization map of BP[7,8] are most sensitive to changes in the concentration of albumins and globulins, which are accompanied by pathological malignant processes of biological tissues of human organs.

Statistical, correlation, and spectral analysis of the orientation-phase structure of BP is promising both for the early detection of oncological diseases of organs and for monitoring their condition during treatment. Thus, the works[6-8] illustrate the differences in the values of estimates of statistical, correlation, and spectral moments of distributions of Mueller matrix images (MMI) of BP and collections of reconstructed orientation and phase maps of BP caused by human gastric cancer. They can be used as a basis for diagnosing gastric cancer, which ranks fourth in the world among malignant tumors..

On the other hand, significant achievements in the last ten years in the development of intelligent technologies and machine learning methods for classification tasks encourage their application in polarization diagnostics systems. Thus, the use of automated decision-making models based on a decision tree[9,10], a convolutional neural network[11-13], or a multilayer perceptron for the classification of MMI and polarization parameters of biological layers has allowed to increase the accuracy of polarization diagnostics. However, these methods require significant amounts of training

*e-mail: natalia.zabolotna@gmail.com

Photonics Applications in Astronomy, Communications, Industry, and High Energy Physics Experiments 2025, edited by Andrzej Smolarz, Ryszard S. Romaniuk, Waldemar Wójcik, Sergii V. Pavlov, Proc. of SPIE Vol. 14009
140090I · © 2025 SPIE · 0277-786X · doi: 10.1117/12.3100539

samples of polarization parameters when diagnosing a specific disease. In their absence and taking into account the fuzzy nature of the existing knowledge bases, preference is given to the principles of forming diagnostic decision-making rules based on fuzzy logic[14–16].

The aim of this work is to increase the diagnostic accuracy of polarization methods for detecting human gastric cancer based on the analysis of the crystal structure of BP by identifying the disease with fuzzy knowledge bases obtained as a result of the reconstruction and analysis of collections of orientational and phase deterministic maps of BP films.

2. ARCHITECTURE OF THE SYSTEM FOR POLARIZATION RECONSTRUCTION AND ANALYSIS OF THE CRYSTAL STRUCTURE OF BLOOD PLASMA IN THE DIAGNOSIS OF GASTRIC CANCER

Taking into account the model of optical polarization properties of BP as a crystal network of globulins and albumins[16], the structure of which is characterized by two-dimensional distributions of orientational $\rho(x,y)$ and phase $\delta(x,y)$ maps, we consider the architecture of the system for experimental reconstruction and analysis of the specified BP parameters (Figure 1).

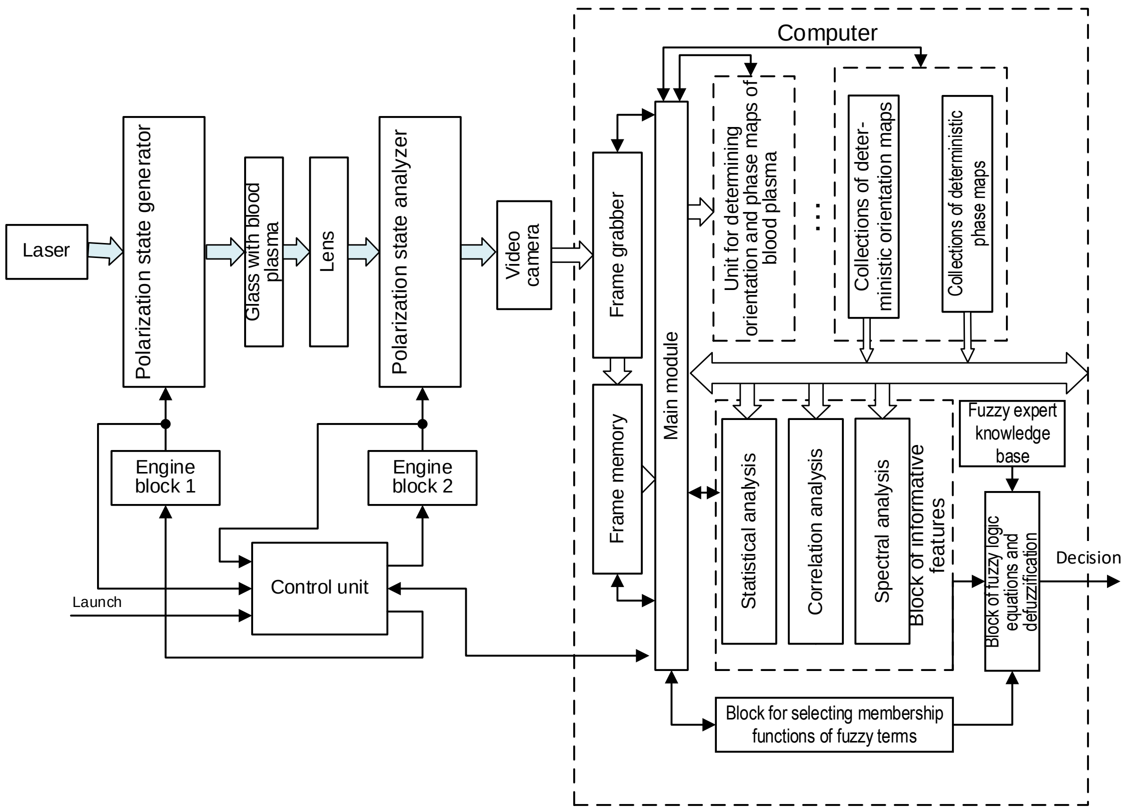

Figure 1. Architecture of the system for polarization reconstruction and analysis of blood plasma structure

The laser generates radiation at a wavelength of 0.638 μm. The laser beam is converted into laser radiation with a given type of polarization using a polarization state generator (PSG) in accordance with the method of measuring the orientation and phase maps of the BP. The formed polarized laser beam is irradiated with blood plasma, applied to transparent laboratory glass and dried at room temperature.

Polarized radiation converted by the blood plasma sample under study enters the polarization state analyzer (PSA) through the lens. It is used to perform polarization filtering of the radiation converted by blood plasma in accordance with the method of measuring orientation and phase maps of BP. The resulting distributions of polarization-filtered radiation intensities are recorded by a digital video camera and transmitted to a computer.

Each of the PSG and PSA blocks includes a polarizer and a quarter-wave phase plate. They can be rotated by a certain angle relative to the corresponding axes and moved in the vertical direction when organizing the selected algorithm for reconstructing maps $\rho(x, y)$ and $\delta(x, y)$. To do this, the system contains engine blocks that are controlled by a control unit.

The methods for direct reconstruction of orientation and phase maps of the BP, implemented in the system in Figure 1, are not presented by the authors in this work; you can read about them in detail in the work[7].

Importantly, the experimentally measured maps $\rho(x, y)$ and $\delta(x, y)$ can be presented as collections of corresponding orientational deterministic maps $\rho(x, y) = const$ and collections of corresponding phase deterministic maps $\delta(x, y) = const$ for BP samples taken from people with the state of "normal" and "gastric cancer" (Figure 2).

Further analysis of the above collections of deterministic maps is analyzed in the system using statistical, correlation, and spectral analysis.

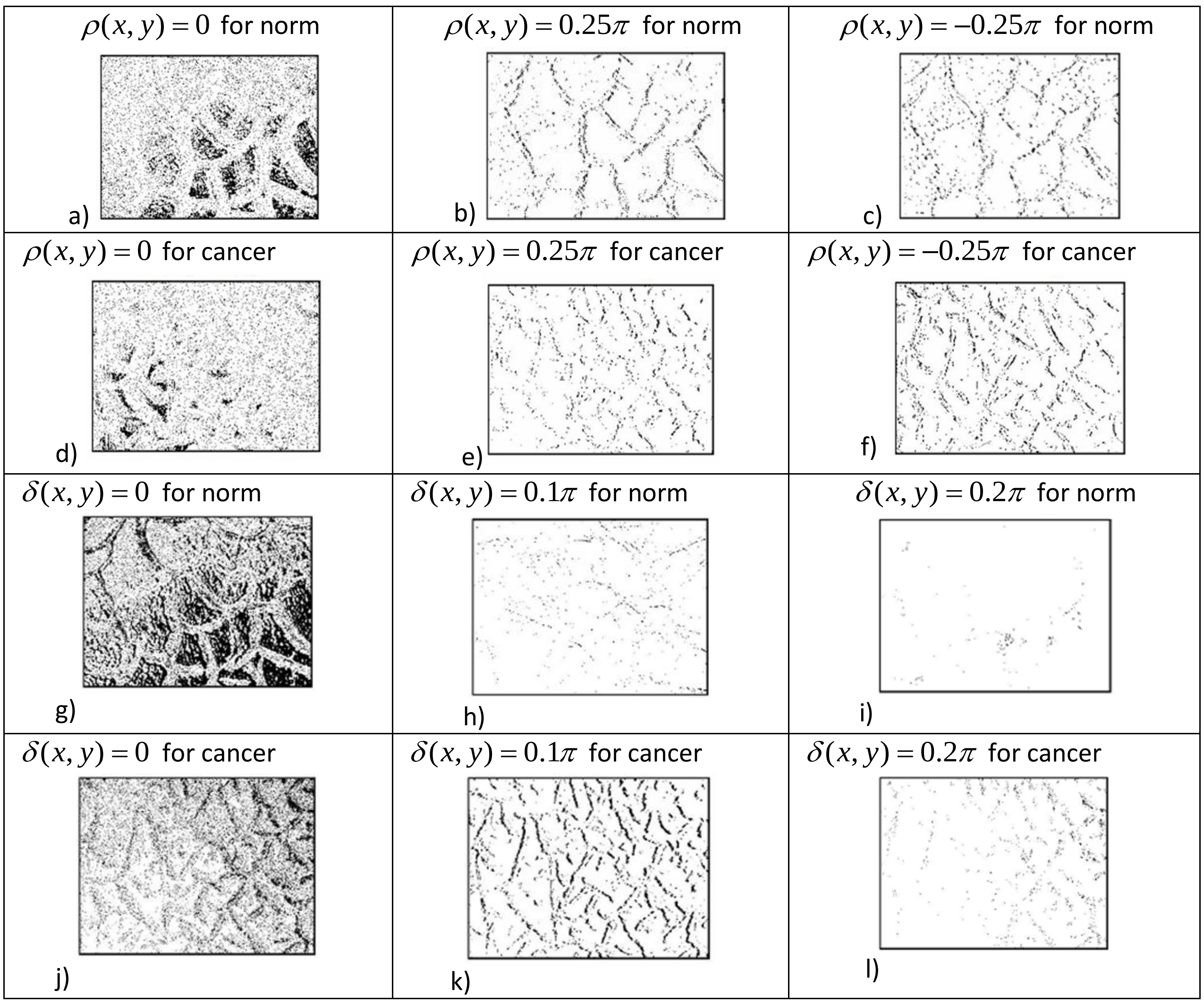

Figure 2. Collections of orientational deterministic maps ((a) – (f)) of BP for the states "normal" ((a), (b), (c)) and "gastric cancer" (d), (e), (f) ; collections of phase deterministic maps ((g) – (l)) of BP for the states "normal" ((g), (h),(i)) and "gastric cancer" (j), (k), (l)

To distribute the elements of each map in the block of informative features, the system determines 4 estimates of the values: statistical moments (A1 – A4); correlation moments (B1 – B4); spectral moments (C1 – C4).

Based on them, the system forms an automated recommended diagnostic solution using a subsystem built on the principles of fuzzy logic. The subsystem uses traditional blocks of such systems: a fuzzy expert knowledge base, a block for selecting membership functions of fuzzy terms, a block of fuzzy logic equations and defuzzification.

3. FUZZY IDENTIFICATION OF GASTRIC CANCER IN THE SYSTEM

The database of researched materials contains 100 samples of BP, represented by 50 samples in the control group "normal" and in the group "gastric cancer". The high sensitivity of the obtained estimates of statistical, correlation and spectral moments of deterministic maps from the collections of BP orientation maps (Table 1) and BP phase maps (Table 2) to changes in the BP crystal structure caused by gastric cancer allowed us to determine the signs of further classification of BP samples in the diagnosis of gastric cancer.

Table 1. Estimates of informative features of collections of orientational deterministic maps of blood plasma taken from representatives of the control group and the “gastric cancer” group

Estimates of features of orientation deterministic maps	Control group			"Gastric cancer" group		
	Collection of orientational deterministic maps			Collection of orientational deterministic maps		
	$\rho = 0$	$\rho = +0.25\pi$	$\rho = -0.25\pi$	$\rho = 0$	$\rho = +0.25\pi$	$\rho = -0.25\pi$
A1	0.424±0.021	0.286±0.017	0.254±0.012	0.350±0.018	0.217±0.013	0.233±0.013
A2	0.212±0.013	0.234±0.011	0.243±0.014	0.178±0.011	0.260±0.011	0.223±0.011
A3	0.754±0.060	1.045±0.063	0.915±0.055	0.886±0.071	1.221±0.073	1.116±0.067
A4	1.385±0.111	1.613±0.093	1.860±0.093	1.550±0.093	1.901±0.110	2.091±0.104
B2	0.257±0.013	0.143±0.007	0.243±0.014	0.245±0.015	0.215±0.010	0.265±0.013
B3	0.405±0.032	1.576±0.095	0.251±0.015	0.526±0.037	0.581±0.034	0.320±0.019
B4	0.864±0.047	3.438±0.189	0.132±0.087	1.112±0.056	0.877±0.043	0.182±0.009
C1	0.693±0.035	0.577±0.040	0.584±0.025	0.645±0.038	0.596±0.035	0.623±0.031
C2	0.169±0.012	0.285±0.002	0.265±0.014	0.222±0.010	0.286±0.017	0.314±0.017
C3	0.095±0.005	0.712±0.042	0.517±0.028	0.116±0.006	0.596±0.029	0.426±0.023
C4	0.134±0.008	0.534±0.032	0.422±0.024	0.186±0.011	0.687±0.039	0.390±0.021

Table 2. Estimates of informative features of collections of phase deterministic maps of blood plasma taken from representatives of the control group and the “gastric cancer” group

Estimates of features of phase deterministic maps	Control group			"Gastric cancer" group		
	Collection of phase deterministic maps			Collection of phase deterministic maps		
	$\delta = 0$	$\delta = +0.1\pi$	$\delta = 0.2\pi$	$\delta = 0$	$\delta = +0.1\pi$	$\delta = 0.2\pi$
A1	0.445±0.027	0.090±0.005	0.052±0.003	0.432±0.022	0.213±0.011	0.160±0.008
A2	0.311±0.022	0.114±0.006	0.093±0.005	0.282±0.014	0.182±0.010	0.184±0.011
A3	0.514±0.035	1.473±0.088	3.143±0.188	0.584±0.029	0.678±0.041	0.861±0.043
A4	0.611±0.030	2.034±0.101	4.777±0.286	0.721±0.041	0.854±0.051	1.183±0.070
B2	0.307±0.015	0.116±0.006	0.060±0.003	0.290±0.014	0.264±0.016	0.212±0.011
B3	0.093±0.006	1.175±0.071	2.812±0.169	0.110±0.005	0.312±0.021	0.530±0.027
B4	0.074±0.004	3.628±0.254	7.766±0.543	0.094±0.006	0.434±0.031	0.545±0.038
C1	0.689±0.048	0.583±0.034	0.512±0.035	0.740±0.005	0.495±0.029	0.344±0.020
C2	0.314±0.016	0.312±0.019	0.266±0.015	0.350±0.017	0.211±0.013	0.132±0.008
C3	0.074±0.004	0.194±0.009	0.310±0.019	0.134±0.008	0.255±0.013	0.720±0.043
C4	0.130±0.009	0.130±0.008	0.224±0.011	0.152±0.010	0.182±0.011	0.684±0.034

The most sensitive informative features were identified among the collections of orientational deterministic maps of BP (Table 3) and among the collections of phase deterministic maps (Table 4) of BP samples taken from representatives of the “normal” group and the “gastric cancer” group. Their peculiarity is that they are represented by a fuzzy knowledge base. The base is formed as a result of representing the corresponding parts of the ranges of changes in informative features using fuzzy terms from “low (L)” to “below average (NA)”, “average (C)”, “above average (AA)”, “high (H)”.

Table 3. Fuzzy knowledge base on informative features of collections of orientational deterministic BP maps for the control group and the "gastric cancer" group

Condition	$C2(\rho=0)$	$C4(\rho=0)$	$B2(\rho=0.25\pi)$	$B2(\rho=0.25\pi)$	$B4(\rho=0.25\pi)$
Norm	L, BA	L, BA	L, BA	AA, H	AA, H
Gastric cancer	AA, H	AA, H	AA, H	L	L

Table 4. Fuzzy knowledge base on informative features of collections of phase deterministic BP maps for the control group and the "gastric cancer" group

Condition	$B3(\delta=0.1\pi)$	$B4(\delta=0.1\pi)$	$B2(\delta=0.2\pi)$	$B3(\delta=0.2\pi)$	$B4(\delta=0.2\pi)$	$C4(\delta=0.2\pi)$
Norm	AA, H	AA, H	L	AA, H	AA, H	L
Gastric cancer	L	L	H	L	L	AA, H

In the future, for the simplicity of writing logical fuzzy equations based on informative features, the notation K_α^β is used, where K is the type of feature (possible types are A, B, C), α is the feature number within the selected type ($\alpha=\overline{1:4}$), β is the angle valueof ρ or δ, depending on the type (orientational or phase) of diagnostics. Then let K_α^β be the membership function $\mu^r(K_\alpha^\beta)$ of one of the five fuzzy terms $(r = L,\ BA,\ M,\ AA,\ H)$ on the interval [0:1].The graphical model of the segment of the membership function is given in . in the article[16]

Below is an example of fuzzy logical equations for membership functions of a collection of phase deterministic BP maps taking into account the fuzzy basis in Table 4. The fuzzy equation for the state “gastric cancer” μ_δ^{cancer} is given in the form of formula (1), the fuzzy equation for the state “normal” μ_δ^{norm} is given in the form of formula (2).

After calculations according to formulas (1) and (2), the maximum value is selected among μ_δ^{cancer} and μ_δ^{norm}, according to which the recommended diagnostic solution for gastric cancer is formed according to phase deterministic BP maps.

By analogy, based on the data in Table 3, fuzzy equations are derived for determining the membership functions μ_ρ^{cancer} and μ_ρ^{norm}, on the basis of which a diagnostic solution is obtained based on the orientational deterministic maps of BP.

$$\mu_\delta^{cancer} = [\mu^L(B_3^{0.1\pi}) \wedge \mu^L(B_4^{0.1\pi}) \wedge \mu^H(B_2^{0.2\pi}) \wedge \mu^L(B_3^{0.2\pi}) \wedge \mu^L(B_4^{0.2\pi}) \wedge \mu^{AA}(C_4^{0.2\pi})] \vee$$
$$[\mu^L(B_3^{0.1\pi}) \wedge \mu^L(B_4^{0.1\pi}) \wedge \mu^H(B_2^{0.2\pi}) \wedge \mu^L(B_3^{0.2\pi}) \wedge \mu^L(B_4^{0.2\pi}) \wedge \mu^H(C_4^{0.2\pi})] \quad (1)$$

$$
\begin{aligned}
&\mu_{\delta}^{norm} = [\mu^{AA}(B_3^{0.1\pi}) \wedge \mu^{AA}(B_4^{0.1\pi}) \wedge \mu^{L}(B_2^{0.2\pi}) \wedge \mu^{AA}(B_3^{0.2\pi}) \wedge \mu^{AA}(B_4^{0.2\pi}) \wedge \mu^{L}(C_4^{0.2\pi})] \vee [\mu^{AA}(B_3^{0.1\pi}) \wedge \\
&\mu^{AA}(B_4^{0.1\pi}) \wedge \mu^{L}(B_2^{0.2\pi}) \wedge \mu^{AA}(B_3^{0.2\pi}) \wedge \mu^{H}(B_4^{0.2\pi}) \wedge \mu^{L}(C_4^{0.2\pi})] \vee [\mu^{AA}(B_3^{0.1\pi}) \wedge \mu^{AA}(B_4^{0.1\pi}) \wedge \mu^{L}(B_2^{0.2\pi}) \wedge \\
&\mu^{H}(B_3^{0.2\pi}) \wedge \mu^{AA}(B_4^{0.2\pi}) \wedge \mu^{L}(C_4^{0.2\pi})] \vee [\mu^{AA}(B_3^{0.1\pi}) \wedge \mu^{AA}(B_4^{0.1\pi}) \wedge \mu^{L}(B_2^{0.2\pi}) \wedge \mu^{H}(B_3^{0.2\pi}) \wedge \mu^{H}(B_4^{0.2\pi}) \wedge \\
&\mu^{L}(C_4^{0.2\pi})] \vee [\mu^{AA}(B_3^{0.1\pi}) \wedge \mu^{H}(B_4^{0.1\pi}) \wedge \mu^{L}(B_2^{0.2\pi}) \wedge \mu^{AA}(B_3^{0.2\pi}) \wedge \mu^{AA}(B_4^{0.2\pi}) \wedge \mu^{L}(C_4^{0.2\pi})] \vee [\mu^{AA}(B_3^{0.1\pi}) \wedge \\
&\mu^{H}(B_4^{0.1\pi}) \wedge \mu^{L}(B_2^{0.2\pi}) \wedge \mu^{AA}(B_3^{0.2\pi}) \wedge \mu^{H}(B_4^{0.2\pi}) \wedge \mu^{L}(C_4^{0.2\pi})] \vee [\mu^{AA}(B_3^{0.1\pi}) \wedge \mu^{H}(B_4^{0.1\pi}) \wedge \mu^{L}(B_2^{0.2\pi}) \wedge \\
&\mu^{H}(B_3^{0.2\pi}) \wedge \mu^{AA}(B_4^{0.2\pi}) \wedge \mu^{L}(C_4^{0.2\pi})] \vee [\mu^{AA}(B_3^{0.1\pi}) \wedge \mu^{H}(B_4^{0.1\pi}) \wedge \mu^{L}(B_2^{0.2\pi}) \wedge \mu^{H}(B_3^{0.2\pi}) \wedge \mu^{H}(B_4^{0.2\pi}) \wedge \\
&\mu^{L}(C_4^{0.2\pi})] \vee [\mu^{H}(B_3^{0.1\pi}) \wedge \mu^{AA}(B_4^{0.1\pi}) \wedge \mu^{L}(B_2^{0.2\pi}) \wedge \mu^{AA}(B_3^{0.2\pi}) \wedge \mu^{AA}(B_4^{0.2\pi}) \wedge \mu^{L}(C_4^{0.2\pi})] \vee [\mu^{H}(B_3^{0.1\pi}) \wedge \\
&\mu^{AA}(B_4^{0.1\pi}) \wedge \mu^{L}(B_2^{0.2\pi}) \wedge \mu^{AA}(B_3^{0.2\pi}) \wedge \mu^{H}(B_4^{0.2\pi}) \wedge \mu^{L}(C_4^{0.2\pi})] \vee [\mu^{H}(B_3^{0.1\pi}) \wedge \mu^{AA}(B_4^{0.1\pi}) \wedge \mu^{L}(B_2^{0.2\pi}) \wedge \\
&\mu^{H}(B_3^{0.2\pi}) \wedge \mu^{AA}(B_4^{0.2\pi}) \wedge \mu^{L}(C_4^{0.2\pi})] \vee [\mu^{H}(B_3^{0.1\pi}) \wedge \mu^{AA}(B_4^{0.1\pi}) \wedge \mu^{L}(B_2^{0.2\pi}) \wedge \mu^{H}(B_3^{0.2\pi}) \wedge \mu^{H}(B_4^{0.2\pi}) \wedge \\
&\mu^{L}(C_4^{0.2\pi})] \vee [\mu^{H}(B_3^{0.1\pi}) \wedge \mu^{H}(B_4^{0.1\pi}) \wedge \mu^{L}(B_2^{0.2\pi}) \wedge \mu^{AA}(B_3^{0.2\pi}) \wedge \mu^{AA}(B_4^{0.2\pi}) \wedge \mu^{L}(C_4^{0.2\pi})] \vee [\mu^{H}(B_3^{0.1\pi}) \wedge \\
&\mu^{H}(B_4^{0.1\pi}) \wedge \mu^{L}(B_2^{0.2\pi}) \wedge \mu^{AA}(B_3^{0.2\pi}) \wedge \mu^{H}(B_4^{0.2\pi}) \wedge \mu^{L}(C_4^{0.2\pi})] \vee [\mu^{H}(B_3^{0.1\pi}) \wedge \mu^{H}(B_4^{0.1\pi}) \wedge \mu^{L}(B_2^{0.2\pi}) \wedge \\
&\mu^{H}(B_3^{0.2\pi}) \wedge \mu^{AA}(B_4^{0.2\pi}) \wedge \mu^{L}(C_4^{0.2\pi})] \vee [\mu^{H}(B_3^{0.1\pi}) \wedge \mu^{H}(B_4^{0.1\pi}) \wedge \mu^{L}(B_2^{0.2\pi}) \wedge \mu^{H}(B_3^{0.2\pi}) \wedge \\
&\mu^{H}(B_4^{0.2\pi}) \wedge \mu^{L}(C_4^{0.2\pi})].
\end{aligned}
\tag{2}
$$

To assess the accuracy of differentiation of the “normal” and “gastric cancer” states in the system shown in Figure 1, an experimental study was conducted on a sample of 100 BP samples, formed by two groups (control group and gastric cancer group) of 50 samples each. The training and test samples of BP samples consisted of 60 and 40 samples, respectively.

The accuracy of diagnosing gastric cancer in the system based on fuzzy identification of a collection of orientational deterministic BP maps was 86%, which is 2.3% higher than in the analogue[7]. An increase in the diagnostic accuracy to 92% was obtained in the system based on fuzzy identification of a collection of phase deterministic BP maps. This is 2.5% better than in the analogue [7].

4. CONCLUSIONS

The method of identifying malignant processes of the human stomach in the system of polarization reconstruction and analysis of the crystal structure of blood plasma by using fuzzy knowledge bases of informative features of orientational and phase maps of BP was improved. An increase in the accuracy of diagnosing gastric cancer to 86% and to 92% was achieved by fuzzy identification of the collection of orientational deterministic BP maps and the collection of phase deterministic BP maps.

REFERENCES

[1] Ushenko, A., G., Pashkovskaya, N., V., Dubolazov, O.,V. et. al., "Mueller matrix images of human biological fluids, " Romanian Reports in Physics 67 (4), pp. 1467–1479 (2015) https://rrp.nipne.ro/2015_67_4/A26.pdf.

[2] Dubolazov, A.,V, Pashkovskaya, N., V, Ushenko, Y., A. et. al. "Birefringence images of polycrystalline films of human urine in early diagnostics of kidney pathology," Appl Opt. 55(12): B85–B90. (2015) https://doi.org/10.1364/AO.55.000B85.

[3] Wójcik, W., et al., "Medical Fuzzy-Expert System for Assessment of the Degree of Anatomical Lesion of Coronary Arteries", *Int. J. Environ. Res. Public Health, 20,* 979 (2023).

[4] Pavlov, S., V. at al., "Multichannel system for recording myocardial electrical activity", Information Technology in Medical Diagnostics II, London : CRC Press, Balkema book, Taylor & Francis Group, 307–314 (2019).

[5] Mintser, O., P., Oliinychenko, B., P. et al., "Differential phase analysis of laser images of a polycrystalline component of blood plasma in diagnostics of pathological changes in mammary gland, " Proc. SPIE 8698, 86980D (2012) doi: 10.1117/12.2019714.

[6] Zabolotna, N. I., Oliinychenko, B. P., Radchenko, K.O. "System of polarization phasometry of polycrystalline blood plasma networks in mammary gland pathology diagnostics" Proc. of SPIE, 9613, 961311 (2015) doi: 10.1117/12.2187383.
[7] Zabolotna, N., I., Sholota V., V., Okarskyi H., H., "Methods and systems of polarization reproduction and analysis of the biological layers structure in the diagnosis of pathologies," Proc. SPIE 11369, 113691S (2020). doi: 10.1117/12.2556542.
[8] Romanyuk, O., N., Pavlov, S., V., Romanyuk, O., V., et al., "A function-based approach to real-time visualization using graphics processing units", Proc. SPIE 11581, 115810E (2020).
[9] Song, Y.,Y. and Lu, Y. "Decision tree methods: applications for classification and prediction, " Shanghai Arch. Psychiatry 27, 130–135 (2015).
[10] Radchenko, K., O., "Intellectualized Mueller-Jones matrix system of laser polarimetry for breast fibroadenoma diagnosis, " Proc. SPIE 10750, Reflection, Scattering, and Diffraction from Surfaces VI, 107500M (4 September 2018); doi: 10.1117/12.2320130.
[11] Qin, Z. et. al. "How convolutional neural network see the world: a survey of convolutional neural network visualization methods," CoRR abs/1804.11191 (2018).
[12] Majumdar A., Lad, J., Tumanova K. et al. (2024), "Machine learning based local recurrence prediction in colorectal cancer using polarized light imaging", *J. Biomed. Opt.* Vol. 29, No. 15, 052915. doi: 10.1117/1.JBO.29.5.052915.
[13] Robinson, D., Hoong, K., Kleijn, W. B. et. all. "Polarimetric imaging for cervical pre-cancer screening aided be machine learning ex vivo studies, " J. Biomed. Opt. Vol. 28(10), 102904 (2023).
[14] Zadeh L., "A. Fuzzy logic: principles, applications, and perspectives. *Proc. SPIE*. 1991. Vol.1468.
[15] Pavlov, S., V., Mezhiievska, I. A., Wójcik W. et al. (2023), "Perspectives of the application of medical information technologies for assessing the risk of anatomical lesion of the coronary arteries", *Science, Technologies,* Innovations. 1(25), pp. 44-55.
[16] Serkova, V., et al., "Medical expert system for assessment of coronary heart disease destabilization based on the analysis of the level of soluble vascular adhesion molecules", Proc. SPIE 10445, 104453O (2017).